Journal of Biomedical Materials Research Part B: Applied Biomaterials

WILEY

Society For Biomaterials

RESEARCH ARTICLE OPEN ACCESS

Resorption Pattern and Bone Regeneration Using a Synthetic Bone Substitute Block With or Without rhBMP-2 and Bisphosphonates: An in Vivo Experiment

Seung Ha Yoo[1] | Young Woo Song[2] | Seung-Hyun Park[1] | Jae-Hong Lim[3] | Ronald Jung[4] | Daniel Thoma[1,4] | Ui-Won Jung[1]

[1]Department of Periodontology, Research Institute for Periodontal Regeneration, Yonsei University College of Dentistry, Seoul, South Korea | [2]Department of Periodontology, Dental Hospital, Veterans Health Service Medical Center, Seoul, South Korea | [3]Pohang Accelerator Laboratory, POSTECH, Pohang, South Korea | [4]Clinic of Reconstructive Dentistry, Center of Dental Medicine, University of Zurich, Zurich, Switzerland

Correspondence: Ui-Won Jung (drjew@yuhs.ac)

Received: 8 October 2025 | **Revised:** 23 April 2026 | **Accepted:** 26 May 2026

Keywords: animal experiment | biocompatible material | bisphosphonate | bone morphogenetic protein-2 | bone regeneration | bone substitutes | preclinical study

ABSTRACT

This study aimed to investigate whether recombinant human bone morphogenetic protein-2 (rhBMP-2) or bisphosphonate added to synthetic block bone substitute influences new bone formation and grafting material degradation patterns. In a rabbit calvarial model, four critical-size bone defects were created and treated with a saline-soaked synthetic bone block (SBB group), bisphosphonate-soaked synthetic bone block (BPS group), rhBMP-2-soaked synthetic bone block (BMP group), or left untreated as control (control group). At 8 weeks, synchrotron-based micro-computed tomography (micro-CT) and histological analyses were performed. All outcomes were evaluated separately in intrabony areas, embedded within the native bone, and extrabony areas, extending beyond the bone surface. Synchrotron-based micro-CT analysis revealed limited resorption of the synthetic bone block across all groups, as the mean percentages of synthetic bone block resorption of the SBB group, BPS group, and BMP group were 8.56%, 11.13%, and 9.11%, respectively, with no significant differences. The cylindric morphology of the grafts was preserved even in the exophytic extrabony portion. Histological evaluation showed that BMP significantly enhanced new bone formation, particularly in the intrabony area (2.65 mm^2 for SBB group, 1.37 mm^2 for BPS group, and 4.41 mm^2 for BMP group in mean). Despite these differences in osteogenic activity, neither bisphosphonate nor rhBMP-2 markedly increased graft resorption, as residual bone graft material was well preserved. Synthetic bone blocks could provide volume stability in both intrabony and extrabony regions, regardless of the addition of bioactive mediators. RhBMP-2 enhanced bone regeneration, though.

1 | Introduction

When ridge augmentation is needed for implant placement, various ways of bone regeneration have been suggested, such as guided bone regeneration, ridge expansion or splitting, and block bone graft [1, 2]. Among these methods, block bone grafting materials are often recommended in case of extensive ridge augmentation with the autogenous bone block being considered as gold standard, due to its osteogenic, osteoinductive and osteoconductive properties without elucidating an immunological rejection [3, 4].

However, the autogenous block bone has limited clinical use accompanied with substantial drawbacks, including limited

Seung Ha Yoo and Young Woo Song contributed equally to this study.

graft volume, donor site morbidity, and unpredictable resorption, reaching up to 50% of the original volume within the first 6 months [5, 6]. Because of these drawbacks, alternatives such as xenogeneic and synthetic block bone substitutes have been developed and studied to achieve comparable regenerative outcomes with minimal burden on patients [7]. Notable advantages thereby include no need for additional donor site surgery, feasibility of being manufactured in desired amount and shape, and maintaining the grafted site volume in a more predictable manner [8].

When compared to the xenogeneic bone block, a synthetic bone block, composed of a mixture of hydroxyapatite and beta-tricalcium phosphate, has an additional benefit of being able to be used without restrictions for patients who have concerns about materials derived from xenografts [9]. The synthetic bone block has proven to be reliable for use in numerous clinical indications, such as horizontal and/or vertical ridge augmentation as well as ridge preservation procedures after tooth extraction [10–12]. Because of its ability to maintain the volume and the augmented space, it might be an appropriate candidate biomaterial as a carrier for bioactive agents.

While most of the previous studies focused on the capacity of synthetic bone particulate or collagenated soft-type block [13–18], the interaction with the hard-type synthetic bone block is still insufficiently understood and requires further investigation. When soaked by various kinds of local agents, such as growth factors or recombinant human bone morphogenetic protein-2 (rhBMP-2), the synthetic bone block is subjected to undergo a varying degree of volume stability and bone regeneration. Therefore, the aim of this preclinical study was to investigate whether rhBMP-2 or bisphosphonate added to synthetic block bone substitute influences new bone formation and grafting material resorption patterns.

2 | Materials and Methods

2.1 | Animals

A total of eight male New Zealand White rabbits (2.5–3.0 kg) were used in this experiment. All rabbits were housed in separate cages under standard laboratory conditions and diet, in accordance with the housing protocol of the Association for Assessment and Accreditation of Laboratory Animal Care International (AAALAC). All procedures, including animal selection, care, preparation for anesthesia, and surgical steps, were approved by the Institutional Animal Care and Use Committee (Yonsei Medical Center, Seoul, Korea; approval number 2024-0098) and conducted in accordance with the Animal Research: Reporting of In Vivo Experiments (ARRIVE) guidelines.

2.2 | Study Design

Four circular bone defects, each 4 mm in diameter, were created in the calvarium of eight rabbits. Each calvarium defect was randomly assigned to one of the following four treatment groups.

- Control group: sham surgery, filled with blood clots only, for spontaneous healing
- Saline-soaked bone block (SBB) group: bone block soaked by normal saline
- Bisphosphonate-soaked bone block (BPS) group: bone block soaked with 12 mg/mL pamidronate for 15 min
- rhBMP-2-soaked bone block (BMP) group: bone block soaked with 0.5 mg/mL rhBMP-2 for 15 min

The rabbits were euthanized at 8 weeks postsurgery for further analyses.

2.3 | Surgical Procedure

General anesthesia was induced in the rabbits by intramuscular injection of a mixture of xylazine hydrochloride (Rompun, Bayer, Leverkusen, Germany) and tiletamine-zolazepam (Zoletil 50, Virbac, Carros, France). The surgical sites were shaved and then disinfected using a 10% povidone-iodine solution (Dongindang, Siheung, South Korea). Local anesthesia with 2% lidocaine hydrochloride (Huons, Seoul, South Korea) was administered along the midline of the cranium, followed by a mid-sagittal incision along the center of the calvaria and full-thickness flap elevation for exposure. Four circular defects, each 4 mm in diameter, were created under saline irrigation using a trephine bur, without damaging the underlying dura mater or brain tissue. Each calvarium defect was randomly assigned to one of the following four treatment groups: control group, SBB group, BMP group, and BPS group. In control group, the defect was filled with the blood clot only, allowing spontaneous healing. In rest of the groups, a synthetic bone block (Osteon 3 Block, Genoss, Suwon, South Korea), composed of 60% hydroxyapatite and 40% β-tricalcium phosphate, in a cylindrical form measuring 4 mm in diameter and 3 mm in height, was used as the graft material. The calcium/phosphorus ratios ranged from 1.5 to 2.0. The bone block was prepared by three-dimensional (3D) printing to fit into the 4-mm-diatmeter circular defect made by trephine bur. In the SBB group, only SBB was placed into the defect, then the fit was checked to ensure there was no movement. In BMP group, the BMP solution was prepared by diluting 0.5 mg of *Escherichia coli*-derived rhBMP-2 (Cowellmedi, Busan, South Korea) in 1000ul of saline to achieve a 0.5 mg/mL rhBMP-2 concentration, and the bone block was then soaked in the solution for 15 min. In BPS group, 1 mL of commercially available injectable formulation of pamidronate disodium hydrate (Panorin Injection, Hanlim, Seoul, Korea) was mixed with 250 μL of saline to make 12 mg/mL solution, and then the bone block was soaked into the solution for 15 min. Bone blocks soaked with each solution were placed into the defect in the same manner. After the materials were inserted, the flap was repositioned to its original position then sutured using absorbable 4–0 suture material (Monosyn, B. Braun, Melsungen, Germany). Representative images of the surgical procedure are shown in Figure 1.

2.4 | Evaluation Method

2.4.1 | Clinical Observation

The surgical sites were carefully monitored for complications such as inflammation, allergic reactions, postoperative bleeding, and infection during the 8 weeks postoperative period.

2.4.2 | Synchrotron-Based Micro-Computed Tomographic Analysis

For volume measurement of synthetic bone blocks of the SBB, BMP, and BPS groups, synchrotron-based micro-computed tomography (micro-CT) was performed at Beamline 6C of Pohang Light Source-II (Pohang Accelerator Laboratory X-ray Electron Laser, Pohang, Korea) [19]. Preoperative cylindrical bone blocks were scanned at 30 keV using a detector setup providing a 4.1 mm x 3.5 mm field of view with a pixel size of 0.65 μm. Throughout scanning, each block was kept immersed in saline solution to ensure preservation. Postoperative bone blocks, each excised and formalin-fixed calvarial specimen after the euthanasia of experimental animals, were mounted in a plastic container immersed in the fixing solution and scanned at 48.5 keV. The detector set-up provided a 7.4 mm × 7.4 mm field of view with a pixel size of 3.2 μm.

CT reconstruction was performed using Octopus 8.7 software (XRE, Ghent, Belgium), which supports filtered backprojection. The resulting 3D images were visualized and analyzed with Amira 2024.1 (Thermo Fisher Scientific, Hillsboro, OR, USA).

Segmentation of the 3D images from both preoperative and postoperative CT datasets was carried out using the watershed algorithm [20]. For volumetric comparison between preoperative and postoperative bone blocks, the datasets were registered using normalized mutual information as the similarity metric [21]. The registration was refined sequentially, beginning with rigid transformation and progressing through iso-scaling, anisoscaling, and shear, followed by a final non-rigid transformation.

To estimate the percentage of synthetic bone blocks resorption (PSR), the post-operative volume of bone block was divided by the pre-operative volume of bone block, and the result was subtracted from 1 to calculate the rate of synthetic bone block volume that underwent the resorption. In addition, the intrabony and extrabony resorption rates (IRR and ERR, respectively) were separately calculated within the portions inside (intrabony area) and outside (extrabony area) of the pristine calvarium defect. The entire method for 3D resorption measurement is described *n* Figure 2.

2.4.3 | Descriptive Histology and Histometric Analysis

The specimens were fixed in 10% formalin for 10 days, then decalcified in 5% formic acid for 14 days, followed by embedding in paraffin. The specimens were then sectioned in the caudocranial direction, along the midline of the defect at a thickness of 5 μm. Hematoxylin–eosin staining and Masson's trichrome staining were performed, and then the specimens were scanned digitally by using a light microscope (DM LB, Leica Microsystems, Wetzlar, Germany), equipped with a camera (DC300F, Leica Microsystems). The slides were then histometrically analyzed using a computer-aided image analysis program (Case Viewer 2.2; 3DHISTECH Ltd., Budapest, Hungary). Histomorphometric measurements were performed

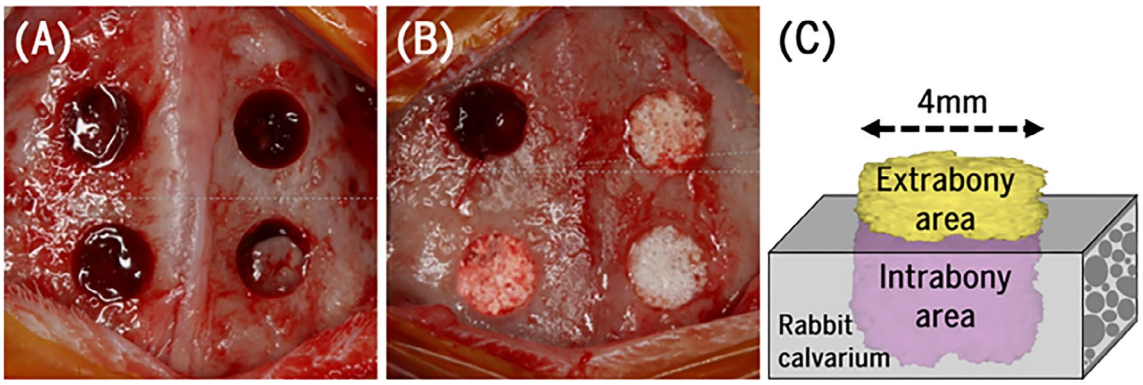

FIGURE 1 | Representative images of surgical procedure. (A) Four defects (⌀ = 4 mm) were created in the calvarium of 8 rabbits. (B) Random assignment of defects: Control group (top left), rhBMP-2-soaked bone block (BMP) group (top right), bisphosphonate-soaked bone block (BPS) group (bottom left), and saline-soaked bone block (SBB) group (bottom right). (B) Diagrammatic representation of the experimental procedure. (C) Schematic illustration describing the surgical site.

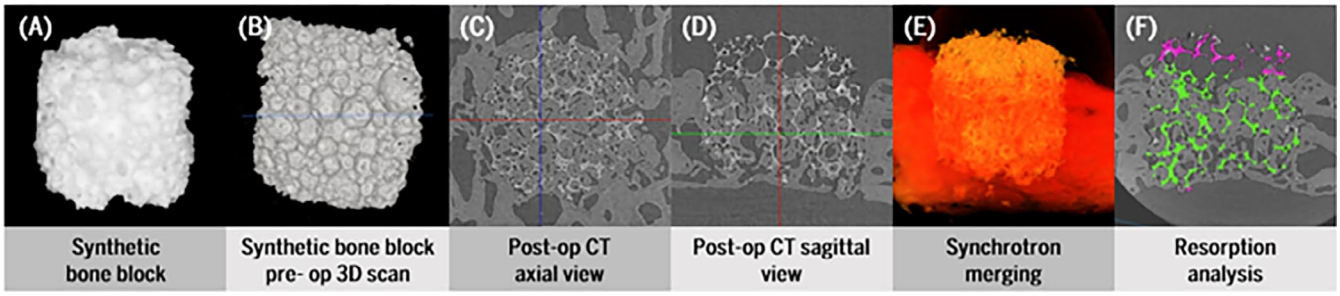

FIGURE 2 | Representative images of synchrotron observation. (A) Preoperative synthetic bone block. (B) 3D scan of the preoperative synthetic bone block. (C) Postoperative CT view (axial). (D) Postoperative CT view (sagittal). (E) Merged preoperative and postoperative scans. (F) Resorption analysis, showing intrabony (green) and extrabony (pink) areas, separately.

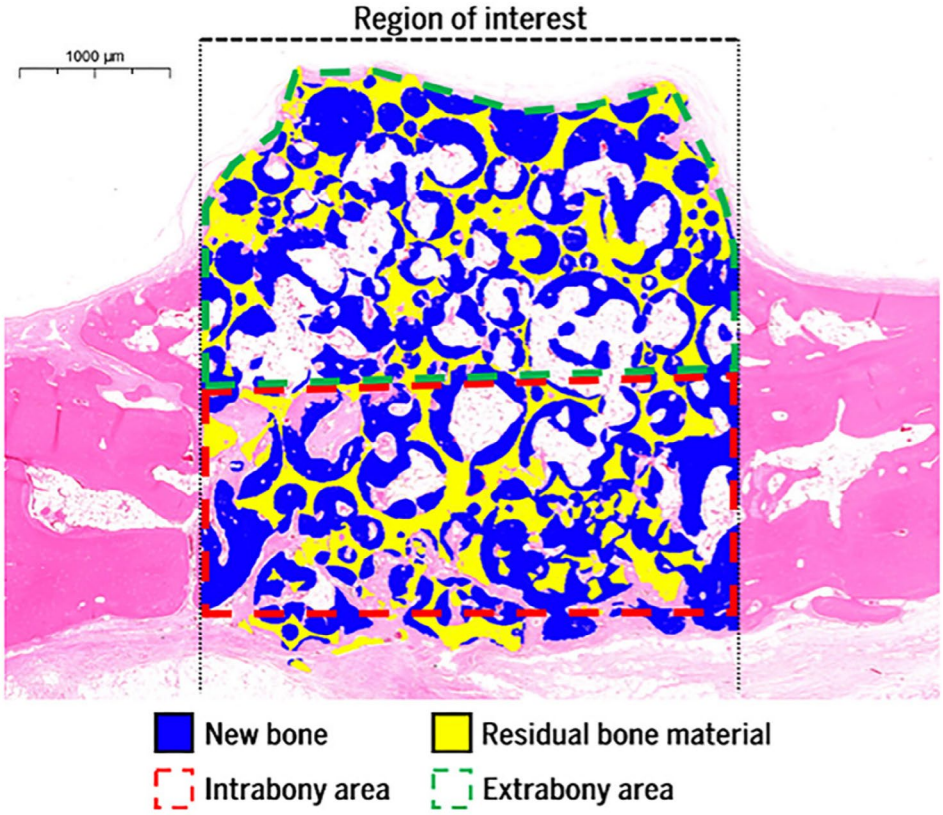

FIGURE 3 | Diagrammatic Representation of the Histomorphometric Analysis Procedure. The outline of the total augmented area is defined as the newly formed bone within the inner part of the block, combined with the bone substitute block area. The blue-colored portion represents the area of newly formed bone area, and the yellow-colored portion shows the area of residual bone materials. The area surrounded by the red-dotted line indicates the intrabony region, while the area surrounded by the green-dotted line indicates the extrabony region.

using a software program (Adobe Photoshop, Adobe Systems), by a single investigator (S.H.Y.) who is experienced and blinded to the group assignment.

For the region of interest (ROI), the lateral defect cuts made by the trephine bur were defined as the lateral border of ROI. The superior border was where the defect or bone block was covered by the soft tissue, and the inferior border was defined by the dura mater. Within the defined ROI, the following three parameters were measured and processed for statistical analysis.

- Total augmented area (TAA; mm^2): the overall area within the ROI including new bone area, residual material area, and fibrovascular connective tissue area.
- New bone area (NBA; mm^2): the area where newly formed bone was observed within the ROI.
- Residual material area (RMA; mm^2): the area where residual graft material was observed within the ROI.

Since there was no graft material applied in the control group, the RMA was estimated only in the SBB, BMP, and BPS groups. Moreover, the NBA and RMA were additionally measured within the extrabony and intrabony portions in the SBB, BMP, and BPS groups. Figure 3 provides an overview on the histomorphometry performed.

2.5 | Statistical Analysis

Because of the exploratory nature of this experiment, no sample size calculation was performed. The statistical analyses were performed using a computer software (SPSS 26, IBM, New York, NY, USA). The data were presented as means [median]. Due to the small sample size, normal distribution was not feasible, so non-parametric tests were applied. The linear mixed model was chosen for the intergroup comparison among the groups, and post hoc analysis was followed if needed. A p value <0.05 was considered statistically significant.

3 | Results

3.1 | Clinical Observations

During the experiment, the surgical sites were clinically observed. None of the rabbits showed signs of infection or other adverse events, including major postoperative complications such as bleeding or swelling during the study period.

3.2 | Synchrotron-Based Micro-CT Analysis

The resorption pattern of the block bone in each group was volumetrically assessed using the synchrotron-based micro-CT

images. The PSR of the SBB group, BPS group, and BMP group was 8.56% [8.26%], 11.13% [11.24%], and 9.11% [7.78%], respectively (Table 1, Figure 4), however, there was no significant difference among the groups. The IRR was 10.34% [11.19%], 10.60% [10.40%], and 9.68% [9.01%], respectively, and the ERR amounted to 7.64% [8.27%], 12.04% [12.29%], and 9.15% [6.79%], respectively. There was no significant difference in both ERR and IRR among the groups ($p < 0.05$).

3.3 | Descriptive Histology

The biological response and tissue integration of the bone blocks were qualitatively investigated using the histologic images. Regardless of the type of biologics applied, all bone blocks demonstrated successful integration with the rabbit calvarial bone. Representative histological images for each group are shown in Figure 5.

On the cellular level, the distribution of osteoclasts and foreign body multinucleated giant cells (FBGCs) was examined histologically. In all four groups, interconnectivity was observed, as the pores of the synthetic bone blocks were connected to each other, allowing newly formed bone to infiltrate within the interconnected pores. Along the surface of the grafting materials, new bone was formed and FBGCs were observed in the surrounding regions. At the border of the region of interest, where the bone graft was in contact with native bone, newly formed bone was in close contact with the native bone, demonstrating stable integration. In the BPS group, FBGCs were predominantly located within the intrabony area. Bone resorption along with new bone formation was evident. In contrast, in the BMP group, only minimal presence of FBGCs was observed within the intrabony area, while FBGCs were primarily observed along the external margins of the bone block. Representative images showing the location of FBGCs in the BPS and BMP groups are illustrated in Figure 6.

3.4 | Histomorphometric Analyses

The histomorphometric analyses allowed providing the quantitative comparison among the groups. All samples grafted with synthetic bone blocks exhibited a significantly greater TAA (12.96 [12.78] mm^2 for SBB group, 12.44 [12.58] mm^2 for BPS group and 13.71 [13.50] mm^2 for BMP group) compared to

TABLE 1 | Synchrotron-based micro-CT analysis: Resorption rate measurements (in percentage).

	SBB			BPS			BMP			
	Mean	Median	95% CI	Mean	Median	95% CI	Mean	Median	95% CI	LMM
PSR	8.56	8.26	(5.83, 11.29)	11.13	11.24	(4.42, 17.84)	9.11	7.78	(5.91, 12.31)	$p = 0.470$
IRR	10.34	11.19	(6.99, 13.69)	10.61	10.40	(4.21, 17.01)	9.68	9.01	(7.44, 11.92)	$p = 0.911$
ERR	7.64	8.27	(4.38, 10.89)	12.04	12.29	(5.06, 19.01)	9.15	6.79	(3.08, 15.21)	$p = 0.261$

Abbreviations: BMP, rhBMP-2-soaked synthetic bone block; BPS, bisphosphonate-soaked synthetic bone block; ERR, extrabony resorption rate; IRR, intrabony resorption rate; LMM, linear mixed model; PSR, percentage of synthetic bone block resorption; SBB, saline-soaked synthetic bone block.

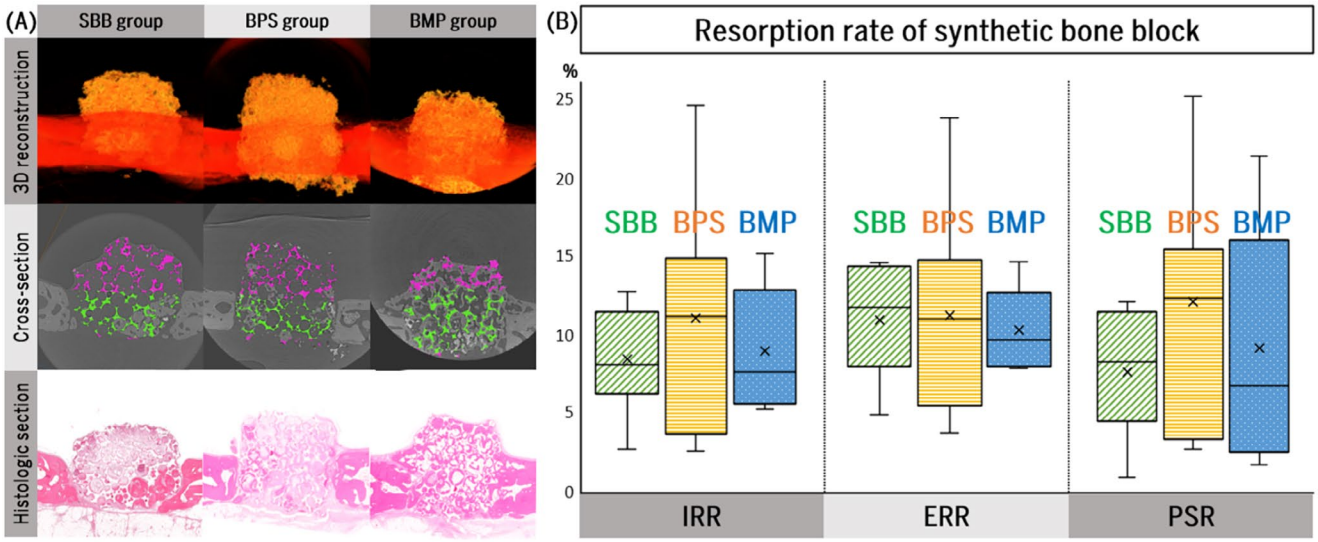

FIGURE 4 | The outcomes of synchrotron-based micro-CT analysis. (A) Representative images of each group. (B) Box and whisker plots of resorption of bone graft material. The *y*-axis represents the percentage of resorption for each group, calculated by dividing the postoperative scanned volume by the preoperative scan volume, subtracting the result from 1, and multiplying by 100. Asterisk (*) indicates statistically significant differences between the blocks. Abbreviations: IRR, intrabony resorption rate; ERR, extrabony resorption rate; PSR, percentage of synthetic bone block resorption; SBB, saline-soaked synthetic bone block; BPS, bisphosphonate-soaked synthetic bone block; BMP, rhBMP-2-soaked synthetic bone block.

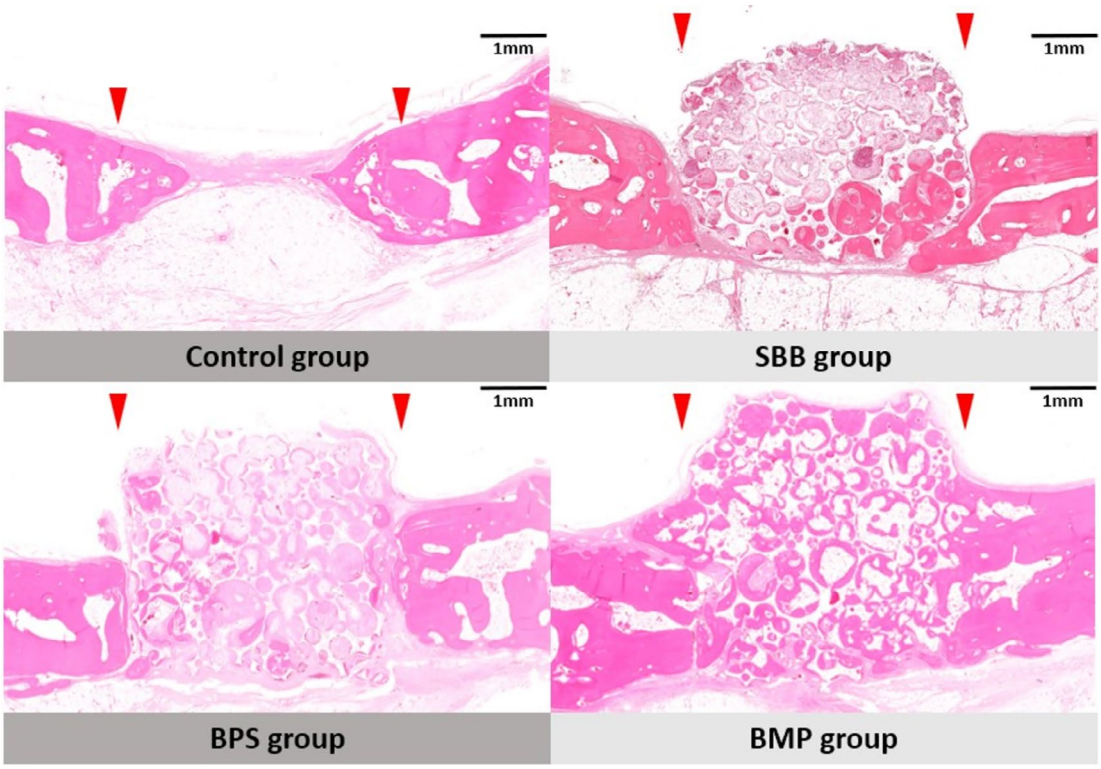

FIGURE 5 | Representative histological image of each group. Red arrow indicates the lateral border of the circular defect. Abbreviations: SBB, saline-soaked synthetic bone block; BPS, bisphosphonate-soaked synthetic bone block; BMP, rhBMP-2-soaked synthetic bone block.

the control group (5.25 [5.27] mm^2, $p < 0.05$). In terms of new bone formation, the BMP group (5.33 [4.85] mm^2, $p < 0.05$) showed significant differences compared to the other groups (1.65 [1.61] mm^2 for control group, 2.89 [2.97] mm^2 for SBB group and 1.68 [1.38] mm^2 for BPS group), while there were no significant differences between control, SBB and the BPS group.

When the SBB, BMP, and BPS groups were compared within each of the intrabony and extrabony area, the BMP group demonstrated higher new bone formation compared to the other two groups; however, the intergroup statistical significance was found only in terms of the intrabony area. The intrabony NBA of the BMP group was 4.41 [4.13] mm^2 followed by those of the SBB group (2.65 [2.76] mm^2) and the BPS group (1.37 [1.17] mm^2) in that order ($p < 0.05$). In the meanwhile, the RMAs were similar among the three groups when compared within either intrabony or extrabony area (Table 2, Figure 7).

4 | Discussion

The present study investigated the efficacy in terms of new bone formation and the pattern of resorption of the synthetic bone block when different types of biologic mediators were added. One of the biologics used in the present experiment, rhBMP-2, is a strong osteoinductive agent, which can promote osteoblast differentiation and subsequently activate bone regeneration [22, 23]. The other one applied was bisphosphonate, which is an osteoclast-inhibiting agent known to prevent bone resorption [24]. The well-known effects of rhBMP-2 and bisphosphonate led to utilizing these two materials to be loaded onto the synthetic bone block in the present study. The obtained results demonstrated that the synthetic bone block was largely preserved in its original cylindric form, with only limited resorption observed across all groups, regardless of whether saline, bisphosphonate, or rhBMP-2 were added. Synchrotron-based micro-CT imaging confirmed that the overall resorption of the blocks remained minimal and did not differ significantly among the groups. Histologically, however, rhBMP-2 promoted more new bone formation, predominantly within the intrabony portion of the graft, while bisphosphonate showed only a modest effect. Despite the different behavior in terms of bone regeneration of the two biologic mediators, the block materials successfully served their role of space maintenance with no evidence of accelerated resorption.

Evaluating the intrabony and extrabony areas separately was thought to be essential to explain healing dynamics and volumetric stability of the graft materials. In the present study, the intrabony area was surrounded by native bone, which resembles the bone substitute grafted within the contained bony defect. The extrabony area was outside of the recipient bed, thereby exposed to the soft tissues and subjected to mechanical pressure, which mimics the clinical situation of bone graft located beyond the bony envelope at the non-contained bony defect. Nevertheless, no differences were found in the pattern of synthetic bone block resorption between intrabony and extrabony areas. This underlines that the synthetic bone block may maintain its volume regardless of the presence of mechanical pressure. This finding aligns with a previous study, where the synthetic bone block was placed without fixation in the rabbit calvaria, and maintained an intact rectangular

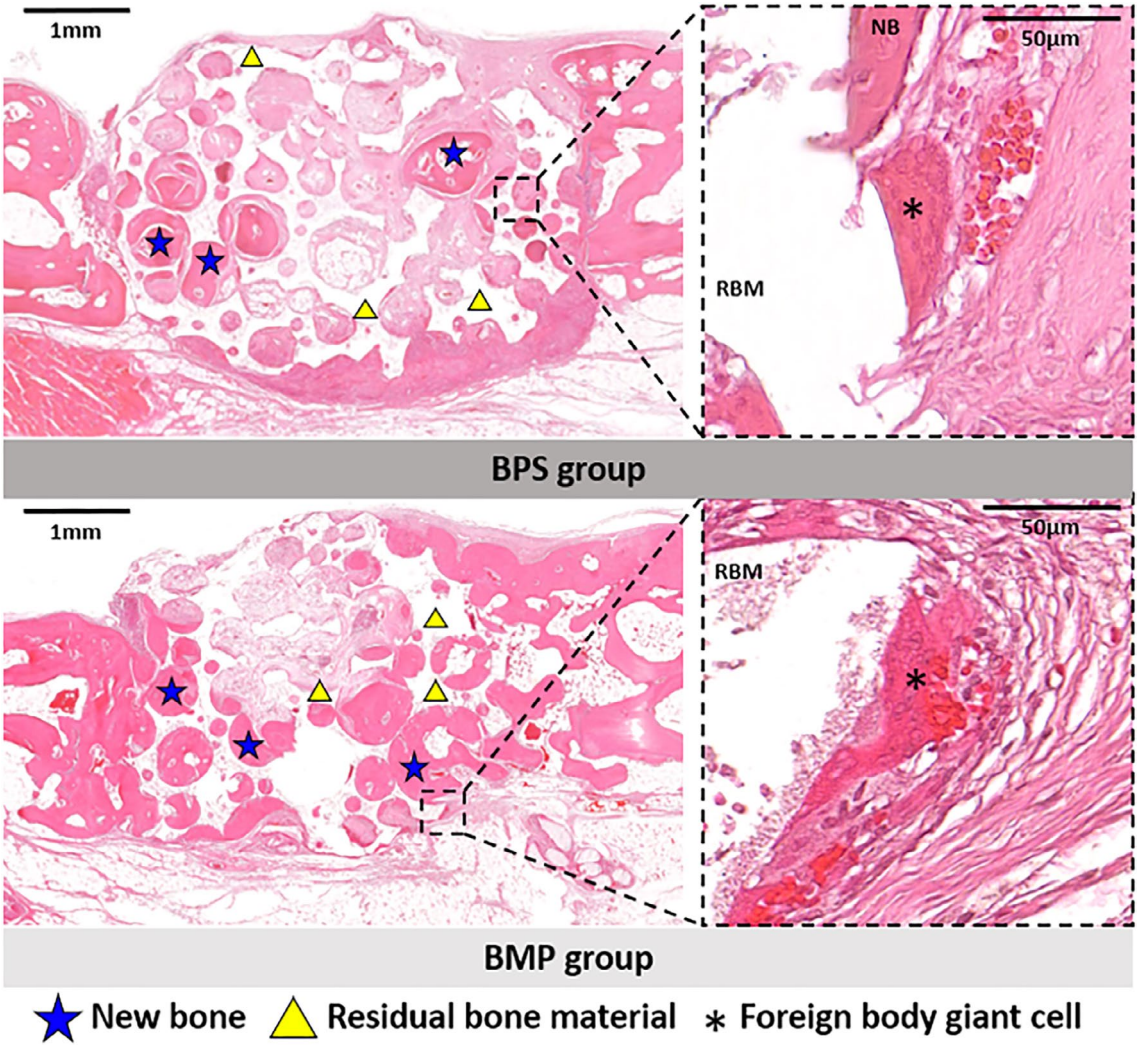

FIGURE 6 | Representative image showing the location of foreign body multinucleated giant cells in the BPS and BMP Groups. The blue star and NB indicate the area of new bone formation, while the yellow triangle and RBM denote the residual bone material area. Asterisk (*) indicates the presence of foreign body multinucleated giant cells. BPS, bisphosphonate-soaked synthetic bone block; BMP, rhBMP-2-soaked synthetic bone block.

shape while the autogenous block graft resulted in a dome-shaped form with distinctive external resorption [25]. The intrabony area showed higher new bone formation compared to the extrabony area across the group, and this might be due to the vascularization potential of two different areas. As the intrabony area was surrounded by native bone, there is greater vascularization potential than at the extrabony area being located outside of the native bone. In summary, the findings imply that if new bone formation is needed outside of the bony envelope, volume maintenance and sufficient blood supply should be guaranteed [26].

For volumetric evaluation, micro-CT had been considered as a traditional method [27]. In this study, synchrotron-based micro-CTs were utilized to quantify volumetric change in intrabony and extrabony areas. This technique has advantages over commonly used micro-CTs, as it uses monochromatic x-ray illumination that can eliminate beam hardening artifact. The synchrotron-based micro-CT measurement of the present study revealed no statistically significant differences between the groups, although the pattern of resorption varied among the groups. In the BMP group, bone resorption appeared to be more active within the center of the grafted volume in the intrabony area, which might reflect accelerated remodeling due to intense osteoinductive signaling [28]. In the BPS group, more active resorption was observed along the external graft margins, the area typically subjected to mechanical pressure.

Histologically, the addition of rhBMP-2 to the synthetic bone block showed a significantly increased new bone formation, compared to the saline and bisphosphonate treated groups. This effect was more prominent in the intrabony area, suggesting that a well-vascularized environment promotes BMP-induced osteogenesis, as the necessary components of osteogenesis such as osteoblast precursor, signaling molecules, and nutrients are supplied to the healing site by blood flow [26]. In addition, the BPS group showed a significantly lower new bone area than the SBB group did, implying that bisphosphonates contribute to the early phase of the healing process by inhibiting osteoclast-mediated bone resorption and the

TABLE 2 | Histomorphometric analysis (in mm^2).

		Control			SBB			BPS			BMP			
		Mean	Median	95% CI	Mean	Median	95% CI	Mean	Median	95% CI	Mean	Median	95% CI	LMM
Total area	TAA	5.25	5.27	(4.31, 6.19)	12.96	12.78	(11.57, 14.34)	12.44	12.58	(11.10, 13.78)	13.71	13.50	(12.89, 14.52)	$p = 0.000$
	Intergroup	**$p = 0.000$ (vs. SBB)**[a]			**$p = 0.000$ (vs. CTL)**[a]			**$p = 0.000$ (vs. CTL)**[a]			**$p = 0.000$ (vs. CTL)**[a]			
	post hoc	**$p = 0.000$ (vs. BPS)**[a]			$p = 1.000$ (vs. BPS)			$p = 1.000$ (vs. SBB)			$p = 1.000$ (vs. SBB)			
	comparison	**$p = 0.000$ (vs. BMP)**[a]			$p = 1.000$ (vs. BMP)			$p = 0.119$ (vs. BMP)			$p = 0.119$ (vs. BPS)			
	NBA	1.65	1.61	(1.00, 2.30)	2.89	2.97	(2.24, 3.54)	1.68	1.38	(0.76, 2.60)	5.33	4.85	(4.30, 6.36)	$p = 0.000$
	Intergroup	$p = 0.174$ (vs. SBB)			$p = 0.174$ (vs. CTL)			$p = 1.000$ (vs. CTL)			**$p = 0.001$ (vs. CTL)**[a]			
	post hoc	$p = 1.000$ (vs. BPS)			$p = 0.159$ (vs. BPS)			$p = 0.159$ (vs. SBB)			**$p = 0.035$ (vs. SBB)**[a]			
	comparison	**$p = 0.001$ (vs. BMP)**[a]			**$p = 0.035$ (vs. BMP)**[a]			**$p = 0.004$ (vs. BMP)**[a]			**$p = 0.004$ (vs. BPS)**[a]			
	RMA	N/A			2.53	2.51	(2.16, 2.90)	2.77	2.54	(2.47, 3.16)	2.82	2.79	(2.47, 3.16)	$p = 0.588$
	Intergroup	N/A			$p = 1.000$ (vs. BPS)			$p = 1.000$ (vs. SBB)			$p = 0.578$ (vs. SBB)			
	post hoc comparison				$p = 0.578$ (vs. BMP)			$p = 1.000$ (vs. BMP)			$p = 1.000$ (vs. BPS)			
Intrabony area	NBA	N/A			2.65	2.76	(1.98, 3.33)	1.37	1.17	(0.65, 2.09)	4.41	4.13	(3.54, 5.29)	$p = 0.000$
	Intergroup	N/A			**$p = 0.033$ (vs. BPS)**[a]			**$p = 0.033$ (vs. SBB)**[a]			**$p = 0.044$ (vs. SBB)**[a]			
	post hoc comparison				**$p = 0.044$ (vs. BMP)**[a]			**$p = 0.002$ (vs. BMP)**[a]			**$p = 0.002$ (vs. BPS)**[a]			
	RMA	N/A			1.40	1.35	(0.95, 1.85)	1.61	1.47	(1.05, 2.18)	1.71	1.7	(1.31, 2.11)	$p = 0.411$
	Intergroup	N/A			$p = 0.954$ (vs. BPS)			$p = 0.954$ (vs. SBB)			$p = 0.610$ (vs. SBB)			
	post hoc comparison				$p = 0.610$ (vs. BMP)			$p = 1.000$ (vs. BMP)			$p = 1.000$ (vs. BPS)			

(Continues)

TABLE 2 | (Continued)

		Control			SBB			BPS			BMP			
		Mean	Median	95% CI	Mean	Median	95% CI	Mean	Median	95% CI	Mean	Median	95% CI	LMM
Extrabony area	NBA		N/A		0.24	0.14	(0.05, 0.42)	0.31	0.21	(0.03, 0.59)	0.92	0.78	(0.43, 1.41)	$p = 0.001$
	Intergroup		N/A		$p = 1.000$ (vs. BPS)			$p = 1.000$ (vs. SBB)			$p = 0.063$ (vs. SBB)			
	post hoc comparison				$p = 0.063$ (vs. BMP)			$p = 0.131$ (vs. BMP)			$p = 0.131$ (vs. BPS)			
	RMA		N/A		1.13	1.16	(0.77, 1.49)	1.16	1.05	(0.78, 1.54)	1.11	1.10	(0.71, 1.50)	$p = 0.973$
	Intergroup		N/A		$p = 1.000$ (vs. BPS)			$p = 1.000$ (vs. SBB)			$p = 1.000$ (vs. SBB)			
	post hoc comparison				$p = 1.000$ (vs. BMP)			$p = 1.000$ (vs. BMP)			$p = 1.000$ (vs. BPS)			

Abbreviations: BMP, rhBMP-2-soaked synthetic bone block; BPS, bisphosphonate-soaked synthetic bone block; LMM, linear mixed model; SBB, saline-soaked synthetic bone block; TAA, total augmented area.
[a]Statistical significance found post hoc (bold).

onset of the osteoblast-mediated bone formation [24, 29]. As the local effect of bisphosphonates decreases over time, physiologic bone remodeling resumes. This might explain the lack of a strong long-term effect on bone formation. This observation is supported by previous studies that used bisphosphonates during the early stage of implant treatment to minimize buccal bone resorption [30].

To further explain the observed healing and resorption patterns, a cellular-level evaluation was conducted, focusing on the distribution of osteoclasts and foreign body multinucleated giant cells (FBGCs). Both osteoclast and FBGCs are monocyte-derived multinucleated cells, but the functions and locations are distinct. In the BPS group, FBGCs were predominantly located within the intrabony area, where bone resorption and new bone formation were actively progressing. This localization may reflect the shift in cellular activity, as the initially bisphosphonate-inhibited osteoclastogenesis was followed by a rebound in resorptive cellular activity as the pharmacologic effect of bisphosphonate vanished. The reactivation of the resorptive activity is consistent with prior studies indicating that bisphosphonates delay but do not eliminate bone remodeling, allowing osteoclast activity to resume after drug withdrawal [31, 32]. In contrast, the BMP group showed a minimal presence of FBGCs within the intrabony area. FBGCs were observed primarily along the external margin of the bone block. This suggests that the bone remodeling and regeneration processes were completed earlier in the intrabony area, as BMP accelerates osteoblast differentiation and early bone matrix deposition [33]. FBGCs were mainly located in the area surrounding the graft materials. However, the appearance of resorptive cells such as FBGCs along the extrabony area raises the question of whether this represents a remodeling activity or a localized inflammatory response.

There are several limitations that must be considered for this study. Firstly, the 8-week observation period may not fully reflect the long-term behavior of synthetic bone blocks under the influence of bioactive agents. The dynamic process of bone remodeling requires a long-term observation to fully understand the resorptive pattern of synthetic bone blocks. Secondly, while the dose of rhBMP-2 was determined based on the previous experiments [34, 35], that of bisphosphonate was chosen in a tentative manner since the previous rabbit calvarial model study which used synthetic bone block as a carrier was scarce. Also, not multiple but only a single concentration of rhBMP-2 and bisphosphonate was tested in this study. As both rhBMP-2 and bisphosphonate are known for their dose-dependent biological effects, future studies should include a range of concentrations to clarify whether dose differences alter the balance between bone formation and graft material resorption. Thirdly, the rabbit calvaria may not fully replicate the clinical conditions involving load-bearing sites or larger augmentation volumes, as it does not reproduce masticatory force. Therefore, future research should be a long-term and dose-dependent study using a clinically relevant experimental model. Such investigation would be essential to establish whether the volume stability of synthetic bone block can be maintained consistently and whether the use of osteogenic or antiresorptive agents could be optimized for improved clinical outcomes.

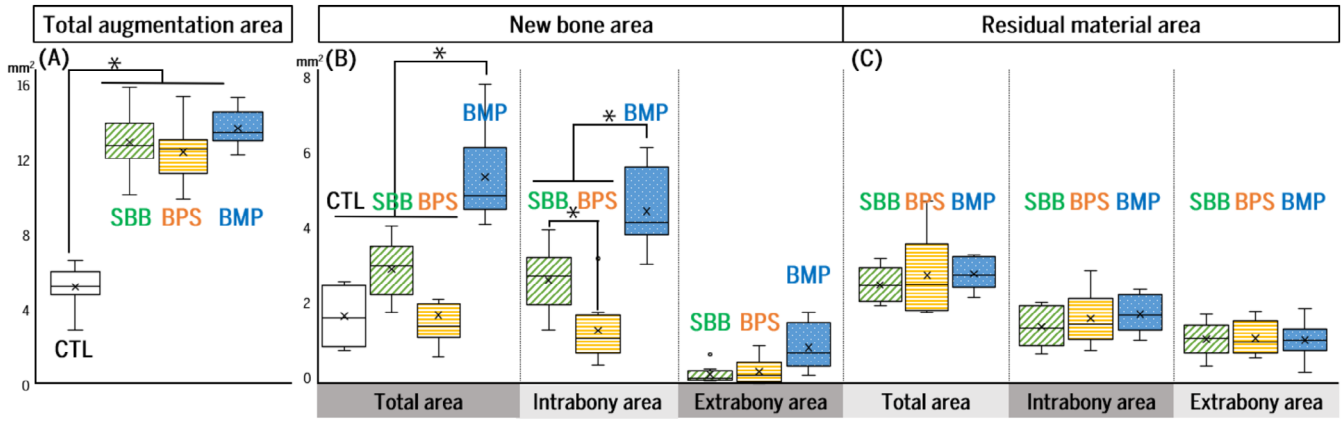

FIGURE 7 | Box and whisker plots of total augmentation area, new bone formation area, and residual bone material area (A, B, C respectively). The y-axis represents the area of each category in mm^2. The "x" inside the box represents the mean value, and the whiskers display the full range of the data. * (bold): Statistical significance found post hoc. Abbreviations: CTL, control group with sham surgery; SBB, saline-soaked synthetic bone block; BPS, bisphosphonate-soaked synthetic bone block; BMP, rhBMP-2-soaked synthetic bone block.

5 | Conclusions

Synthetic bone block provided volume stability regardless of whether saline, rhBMP-2, or bisphosphonate was soaked, and the resorption tendency was similar between the intrabony and extrabony portions. Irrespective of the type of biologics applied, new bone formation within the intrabony portion was more prominent than that within the extrabony portion. RhBMP-2 potentially showed the enhancement of bone regeneration, though.

Author Contributions

Ui-Won Jung: conceptualization. **Ui-Won Jung:** methodology. **Young Woo Song:** investigation. **Seung Ha Yoo**, **Jae-Hong Lim:** formal analysis (lead and supporting). **Seung Ha Yoo:** data curation. **Seung Ha Yoo**, **Jae-Hong Lim:** visualization (lead and supporting). **Seung Ha Yoo**, **Young Woo Song:** writing – original draft (equal). **Ui-Won Jung**, **Jae-Hong Lim**, **Seung-Hyun Park**, **Ronald Jung**, **Daniel Thoma:** writing – review and editing (supporting). **Ui-Won Jung**, **Young Woo Song:** supervision (lead and supporting). **Ui-Won Jung:** funding acquisition.

Acknowledgments

The authors gratefully acknowledge Mr. Seob-Gu Kim for his technical assistance in the segmentation and registration of CT images. Experiments at beamline 6C of PLS-II were supported by the Korean Ministry of Science and ICT (MIST) and POSTECH. This work was supported by the National Research Foundation of Korea (NRF) grant funded by the Korea government (MSIT) (RS-2026-25469650).

Funding

This work was supported by the National Research Foundation of Korea (NRF) grant funded by the Korea government (MSIT) (RS-2026-25469650).

Conflicts of Interest

The authors declare no conflicts of interest.

Data Availability Statement

The data that support the findings of this study are available from the corresponding author upon reasonable request.

References

1. G. Gurler, C. Delilbasi, H. Garip, and S. Tufekcioglu, "Comparison of Alveolar Ridge Splitting and Autogenous Onlay Bone Grafting to Enable Implant Placement in Patients With Atrophic Jaw Bones," *Saudi Medical Journal* 38, no. 12 (2017): 1207–1212.

2. I. A. Urban, E. Montero, E. Amerio, D. Palombo, and A. Monje, "Techniques on Vertical Ridge Augmentation: Indications and Effectiveness," *Periodontology 2000* 93, no. 1 (2023): 153–182.

3. H. V. Precheur, "Bone Graft Materials," *Dental Clinics of North America* 51, no. 3 (2007): 729–746.

4. L. Trombelli, L. J. Heitz-Mayfield, I. Needleman, D. Moles, and A. Scabbia, "A Systematic Review of Graft Materials and Biological Agents for Periodontal Intraosseous Defects," *Journal of Clinical Periodontology* 29, no. 3 (2002): 117–135.

5. M. A. Jardini, A. C. De Marco, and L. A. Lima, "Early Healing Pattern of Autogenous Bone Grafts With and Without e-PTFE Membranes: A Histomorphometric Study in Rats," *Oral Surgery, Oral Medicine, Oral Pathology, Oral Radiology, and Endodontology* 100, no. 6 (2005): 666–673.

6. C. M. ten Bruggenkate, H. A. Kraaijenhagen, W. A. van der Kwast, G. Krekeler, and H. S. Oosterbeek, "Autogenous Maxillary Bone Grafts in Conjunction With Placement of I.T.I. Endosseous Implants. A Preliminary Report," *International Journal of Oral and Maxillofacial Surgery* 21, no. 2 (1992): 81–84.

7. G. I. Benic, M. J. Joo, S. R. Yoon, J. K. Cha, and U. W. Jung, "Primary Ridge Augmentation With Collagenated Xenogenic Block Bone Substitute in Combination With Collagen Membrane and rhBMP-2: A Pilot Histological Investigation," *Clinical Oral Implants Research* 28, no. 12 (2017): 1543–1552.

8. G. Zimmermann and A. Moghaddam, "Allograft Bone Matrix Versus Synthetic Bone Graft Substitutes," *Injury* 42, no. 2 (2011): S16-21.

9. H. C. Lim, K. W. Paeng, U. W. Jung, and G. I. Benic, "Effectiveness of Xenogeneic and Synthetic Bone-Block Substitute Materials With/Without Recombinant Human Bone Morphogenetic Protein-2: A Preclinical Study Using a Rabbit Calvarium Model," *Journal of Clinical Periodontology* 48, no. 8 (2021): 1126–1136.

10. S. Park, J. Y. Lee, J. Y. Park, et al., "Ridge Augmentation Using a Self-Retaining Block Bone Material in Damaged Extraction Sockets: A Multi-Centre Randomized Controlled Clinical Trial," *Journal of Clinical Periodontology* 52, no. 4 (2025): 599–611.

11. J. Y. Park, J. Y. Lee, S. Park, J. K. Cha, J. S. Lee, and U. W. Jung, "Synchrotron Analysis of Damaged Extraction Sockets Augmented Using a

Synthetic Bone Block: A Pilot Study," *International Journal of Periodontics & Restorative Dentistry* 44, no. 3 (2024): 299–307.

12. Y. H. Kwon, Y. W. Song, J. Y. Park, et al., "Ridge Preservation Using a Self-Retaining Block Type Bone Substitute for Extraction Sockets With Buccal Dehiscence Defects - A Preclinical Study," *Clinical Oral Implants Research* 35, no. 3 (2024): 330–339.

13. J. W. Jang, J. H. Yun, K. I. Lee, et al., "Osteoinductive Activity of Biphasic Calcium Phosphate With Different rhBMP-2 Doses in Rats," *Oral Surgery, Oral Medicine, Oral Pathology, Oral Radiology* 113, no. 4 (2012): 480–487.

14. S. Han, K. W. Paeng, S. Park, U. W. Jung, J. K. Cha, and J. Hong, "Programmed BMP-2 Release From Biphasic Calcium Phosphates for Optimal Bone Regeneration," *Biomaterials* 272 (2021): 120785.

15. J. H. Hwang, S. Oh, and S. Kim, "Improvement of the Osteogenic Potential of ErhBMP-2-/EGCG-Coated Biphasic Calcium Phosphate Bone Substitute: In Vitro and in Vivo Activity," *Journal of Periodontal & Implant Science* 49, no. 2 (2019): 114–126.

16. J. S. Kim, J. K. Cha, A. R. Cho, et al., "Acceleration of Bone Regeneration by BMP-2-Loaded Collagenated Biphasic Calcium Phosphate in Rabbit Sinus," *Clinical Implant Dentistry and Related Research* 17, no. 6 (2015): 1103–1113.

17. D. Gan, M. Liu, T. Xu, K. Wang, H. Tan, and X. Lu, "Chitosan/Biphasic Calcium Phosphate Scaffolds Functionalized With BMP-2-Encapsulated Nanoparticles and RGD for Bone Regeneration," *Journal of Biomedical Materials Research Part A* 106, no. 10 (2018): 2613–2624.

18. Z. Wang, K. Wang, X. Lu, et al., "BMP-2 Encapsulated Polysaccharide Nanoparticle Modified Biphasic Calcium Phosphate Scaffolds for Bone Tissue Regeneration," *Journal of Biomedical Materials Research Part A* 103, no. 4 (2015): 1520–1532.

19. S. J. Seo, J. H. Lim, Y. Lee, C. W. Bark, and Y. G. Kim, "High-Throughput Analysis of New Bone Formation and Bone Substitutes After Maxillary Sinus Floor Elevation Using Synchrotron Radiation Micro-Computed Tomography," *Journal of Nanoscience and Nanotechnology* 19, no. 2 (2019): 680–686.

20. L. Vincent and P. Soille, "Watersheds in Digital Spaces: An Efficient Algorithm Based on Immersion Simulations," *IEEE Transactions on Pattern Analysis & Machine Intelligence* 13, no. 6 (1991): 583–598.

21. J. P. Pluim, J. A. Maintz, and M. A. Viergever, "Mutual-Information-Based Registration of Medical Images: A Survey," *IEEE Transactions on Medical Imaging* 22, no. 8 (2003): 986–1004.

22. P. H. Gomes-Ferreira, R. Okamoto, S. Ferreira, D. De Oliveira, G. A. Momesso, and L. P. Faverani, "Scientific Evidence on the Use of Recombinant Human Bone Morphogenetic Protein-2 (rhBMP-2) in Oral and Maxillofacial Surgery," *Oral and Maxillofacial Surgery* 20, no. 3 (2016): 223–232.

23. C. H. Chung, Y. K. Kim, J. S. Lee, U. W. Jung, E. K. Pang, and S. H. Choi, "Rapid Bone Regeneration by *Escherichia coli*-Derived Recombinant Human Bone Morphogenetic Protein-2 Loaded on a Hydroxyapatite Carrier in the Rabbit Calvarial Defect Model," *Biomaterials Research* 19 (2015): 17.

24. P. R. Jensen, T. L. Andersen, P. Chavassieux, J. P. Roux, and J. M. Delaisse, "Bisphosphonates Impair the Onset of Bone Formation at Remodeling Sites," *Bone* 145 (2021): 115850.

25. S. Y. Bae, J. C. Park, H. S. Shin, Y. K. Lee, S. H. Choi, and U. W. Jung, "Tomographic and Histometric Analysis of Autogenous Bone Block and Synthetic Hydroxyapatite Block Grafts Without Rigid Fixation on Rabbit Calvaria," *Journal of Periodontal & Implant Science* 44, no. 5 (2014): 251–258.

26. M. Marenzana and T. R. Arnett, "The Key Role of the Blood Supply to Bone," *Bone Research* 1, no. 3 (2013): 203–215.

27. H. Z. Lyu and J. H. Lee, "Correlation Between Two-Dimensional Micro-CT and Histomorphometry for Assessment of the Implant Osseointegration in Rabbit Tibia Model," *Biomaterials Research* 25, no. 1 (2021): 11.

28. L. J. Raggatt and N. C. Partridge, "Cellular and Molecular Mechanisms of Bone Remodeling," *Journal of Biological Chemistry* 285, no. 33 (2010): 25103–25108.

29. J. Y. Choi, H. J. Kim, Y. C. Lee, et al., "Inhibition of Bone Healing by Pamidronate in Calvarial Bony Defects," *Oral Surgery, Oral Medicine, Oral Pathology, Oral Radiology, and Endodontics* 103, no. 3 (2007): 321–328.

30. I. Hong, J. M. Joo, Y. H. Kwon, et al., "Local Delivery of Pamidronate With Collagen Matrix Mitigates Buccal Bone Resorption Following Immediate Implant Placement - An Experimental in Vivo Study," *Journal of Periodontal Research* 60, no. 3 (2025): 255–264.

31. R. K. Fuchs, R. J. Phipps, and D. B. Burr, "Recovery of Trabecular and Cortical Bone Turnover After Discontinuation of Risedronate and Alendronate Therapy in Ovariectomized Rats," *Journal of Bone and Mineral Research* 23, no. 10 (2008): 1689–1697.

32. Y. Park, T. Sato, and J. Lee, "Functional and Analytical Recapitulation of Osteoclast Biology on Demineralized Bone Paper," *Nature Communications* 14, no. 1 (2023): 8092.

33. M. L. Zou, Z. H. Chen, Y. Y. Teng, et al., "The Smad Dependent TGF-β and BMP Signaling Pathway in Bone Remodeling and Therapies," *Frontiers in Molecular Biosciences* 8 (2021): 593310.

34. S. M. Chung, I. K. Jung, B. H. Yoon, B. R. Choi, D. M. Kim, and J. S. Jang, "Evaluation of Different Combinations of Biphasic Calcium Phosphate and Growth Factors for Bone Formation in Calvarial Defects in a Rabbit Model," *International Journal of Periodontics & Restorative Dentistry* 36 (2016): s49–s59.

35. A. Arias-Betancur, N. Badilla-Wenzel, Á. Astete-Sanhueza, N. Farfán-Beltrán, and F. J. Dias, "Carrier Systems for Bone Morphogenetic Proteins: An Overview of Biomaterials Used for Dentoalveolar and Maxillofacial Bone Regeneration," *Japanese Dental Science Review* 58 (2022): 316–327.